eng

MDPI

Article

Redesign of a Failed Hoisting Shaft of a Vertical Transfer Device

Filipe Alexandre Couto da Silva [1] and Paulo M. S. T. de Castro [2,*]

[1] Departamento de Engenharia Mecânica, Instituto Superior de Engenharia do Porto—ISEP, Instituto Politécnico do Porto, Rua Dr. António Bernardino de Almeida, 4249-015 Porto, Portugal; fcs@isep.ipp.pt

[2] Faculdade de Engenharia, Universidade do Porto, Rua Dr. Roberto Frias, 4200-465 Porto, Portugal

* Correspondence: ptcastro@fe.up.pt

Abstract: The redesign of a failed hoisting shaft belonging to a 10 m stroke vertical transfer device (VTD) is presented. Firstly, the operation of the VTD is thoroughly analysed, the variation of loads and moments along the operating cycle is characterised, and transients such as emergency stop loads are calculated. The selection of safety factors and duty cycle factors was followed by the shaft sizing. After an initial rough sizing, the high-cycle fatigue (HCF) design for cyclic bending moments was performed, first considering constant torque and then considering cyclic torque. The number of bending and torsion cycles performed by the hoisting shaft over 10 years was shown to exceed 10^6, and an infinite life design is mandatory. The analyses showed that the initial shaft diameter was insufficient, thus justifying the failures observed before the present redesign. A classical fatigue model combining torsional shear stresses with bending stresses was used to take into account reversed torsional loading and ensure infinite fatigue life. This work highlights the need to thoroughly understand a machine's operating cycle so that the wrong premises for fatigue design calculations are not assumed.

Keywords: fatigue; machine elements; redesign; shafts; VTD

check for updates

Citation: da Silva, F.A.C.; de Castro, P.M.S.T. Redesign of a Failed Hoisting Shaft of a Vertical Transfer Device. *Eng* **2023**, *4*, 1981–2002. https://doi.org/10.3390/eng4030112

Academic Editor: Antonio Gil Bravo

Received: 13 June 2023
Revised: 10 July 2023
Accepted: 11 July 2023
Published: 14 July 2023

1. Introduction

The present case study concerns a vertical transfer device (VTD) hoisting shaft failure and redesign. The shaft steel is 34CrNiMo6. The size of the machine is suggested by the hoisting stroke—10 m. The machine operation began in 2017, and until 2019, malfunctions of the upper sprocket assembly were reported by the customer. During that period, the hoisting shaft fractured and was replaced by another equal in size and material. Sometime after this replacement, the customer noticed an abnormal play between the shaft and the sprocket on the key area. At the beginning of 2019, it was decided to investigate the root cause of this abnormal behaviour. At the end of 2019, the upper sprocket assembly was replaced by a redesigned one according to the conclusions of the present document, and no more problems were found since this intervention.

The service loads acting upon hoisting shafts typically lead to a number of cycles in excess of 10^7, implying fatigue design for infinite life under rotating bending and torsional loading.

The need for a thorough understanding of the machine operating cycle, so that wrong premises are not assumed for the fatigue design calculations, is emphasised in this paper.

Stress-based high-cycle fatigue (HCF) considerations are used throughout the work, and a classical approach to fatigue was adopted. Harris and Jur recall in [1] that 'the long-taught classical methodology is useful and accurate as both a design and an analysis tool'. The classical fatigue methodology is presented in many references, e.g., Childs [2,3], Beswarick [4,5] or D'Angelo [6], and is widely used in industry, for design as well as for failure analyses, where interpretation of failure causes and redesign of failed parts are objectives to be pursued [7].

Milela [8] or Lee et al. [9] present comprehensive overviews of fatigue, and discuss research on biaxial fatigue as experienced in situations of combined bending and torsion moments, typical of shafts. A survey of recent trends of multiaxial fatigue is given by Anes et al. [10]. Although shaft fatigue is the object of continued research efforts, in the present work, the classical approach commonly used in industry was used for the redesign of a failed shaft subjected to high-cycle fatigue (HCF). Early presentations of the subject are found in, e.g., d'Isa [11], Hall et al. [12] or Spotts [13].

The paper is organized as follows: the VTD operation mode is thoroughly analysed and modelled in Section 2, as a starting point for the hoisting shaft redesign. After a presentation of the VTD mode of operation, the radial load, bending and torsional moments variations along the operating cycle are evaluated, and transients as emergency stop loads are characterized, leading to the inputs for the design calculations and selection of safety and duty cycle factors, as discussed in Section 3.

Using the static failure criterion, a first sizing for the peak load is presented in Section 4. Then, using the normal operation loads calculated in Section 5, a fatigue design using different approaches is presented in Sections 6–8.

The areas with keyseats are particularly sensitive in fatigue calculation. The use of steels with higher tensile strength does not proportionally increases the fatigue allowable in keyseat areas.

Given the organization of the work, relevant references are introduced and discussed throughout the text, as needed. Due to the large number of variables considered, their definitions are given in the Nomenclature of the document, and/or when called for in the text.

2. Detailed Analysis of the Vertical Transfer Device Operation Cycle

Vertical transfer devices are under the scope of the standard EN 619:2002+A1:2010 [14] (EN 619:2002+A1:2010 has a new edition in 2022, not yet harmonised; only the harmonised standards can be used to demonstrate that products comply with the relevant European legislation), where the machine safety requirements are defined. According to this standard, a VTD is a device with raising and lowering movements of more than 200 mm in the path of conveyors, in which unit loads (in logistics terminology, a unit load corresponds to the pallet plus the handled goods) can be transferred from one defined level to one or more defined levels by a carrying element. The hoisting system of the VTD analysed is composed of a driving motorized sprocket on the bottom and a driven sprocket on the top. The suspension consists of one chain that is anchored to the hoisting carriage on one side and a counterweight on the other side; refer to Figure 1 for more details. One conveyor is assembled on the hoisting carriage, and it is responsible for the transfer of the unit load to the grounded conveyors on each transfer level.

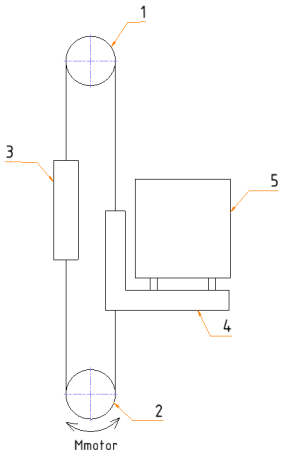

Figure 1. VTD working scheme: 1—upper chain sprocket (driven); 2—bottom chain sprocket (driving); 3—counterweight; 4—hoisting carriage with load handling device; 5—unit load.

In this VTD, the hoisting stroke is 10 m, and the operating cycle consists of the steps described in Figure 2, repeated 24 h/day. Figure 3 presents the evolution of the VTD carriage hoisting speed (m/s) with time (s).

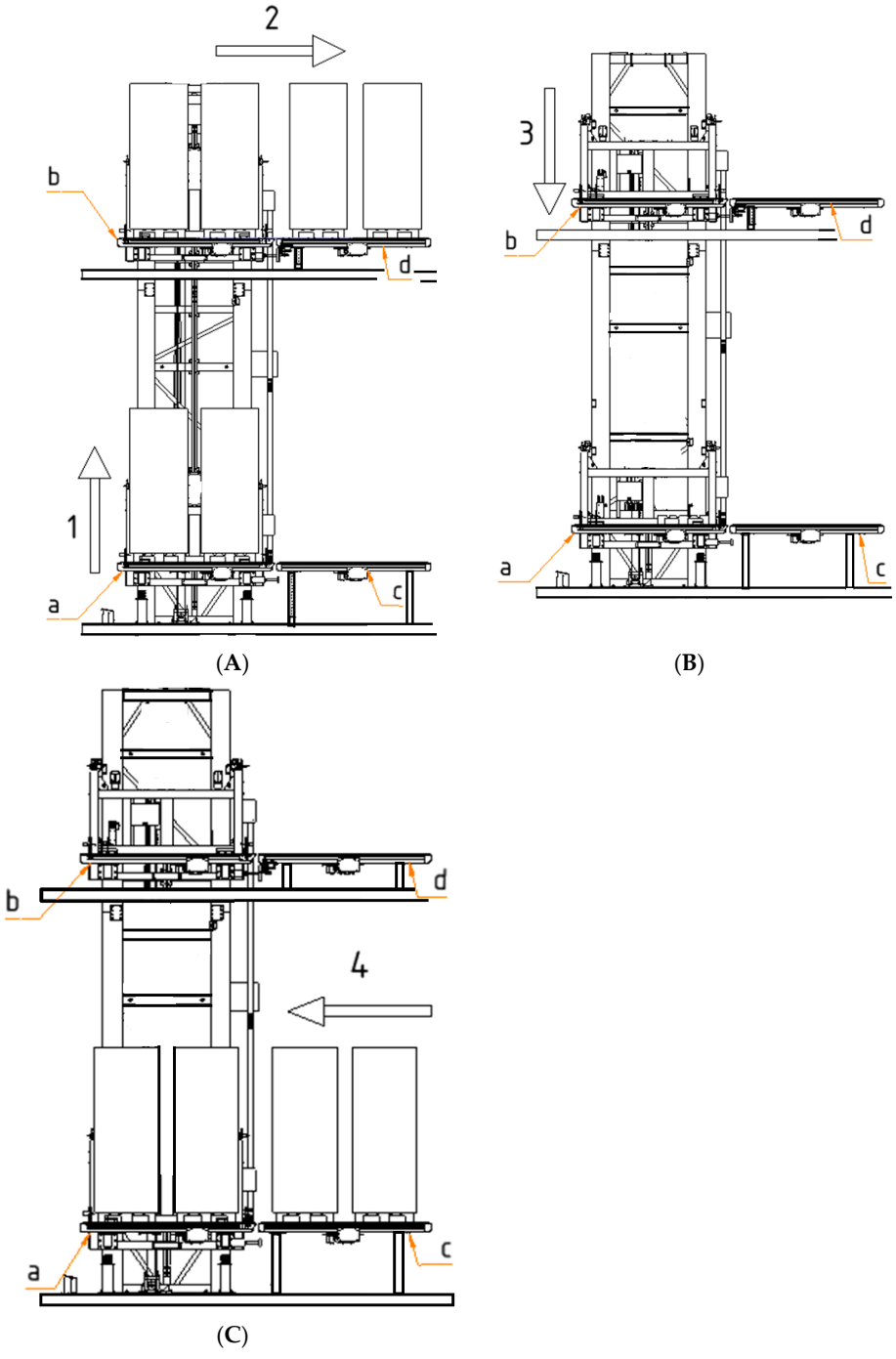

Figure 2. VTD operating cycle. (**A**) Movements 1 and 2. Hoisting and load transfer on the upper level. (**B**) Movement 3. Downward movement from the upper level to level zero. (**C**) Movement 4. Transfer of the unit load from the grounded conveyor to the conveyor mounted on the hoisting carriage: a—conveyor mounted on the VTD hoisting carriage—level zero; b—conveyor mounted on the VTD hoisting carriage—upper level; c—grounded conveyor on level zero; d—grounded conveyor on the upper level.

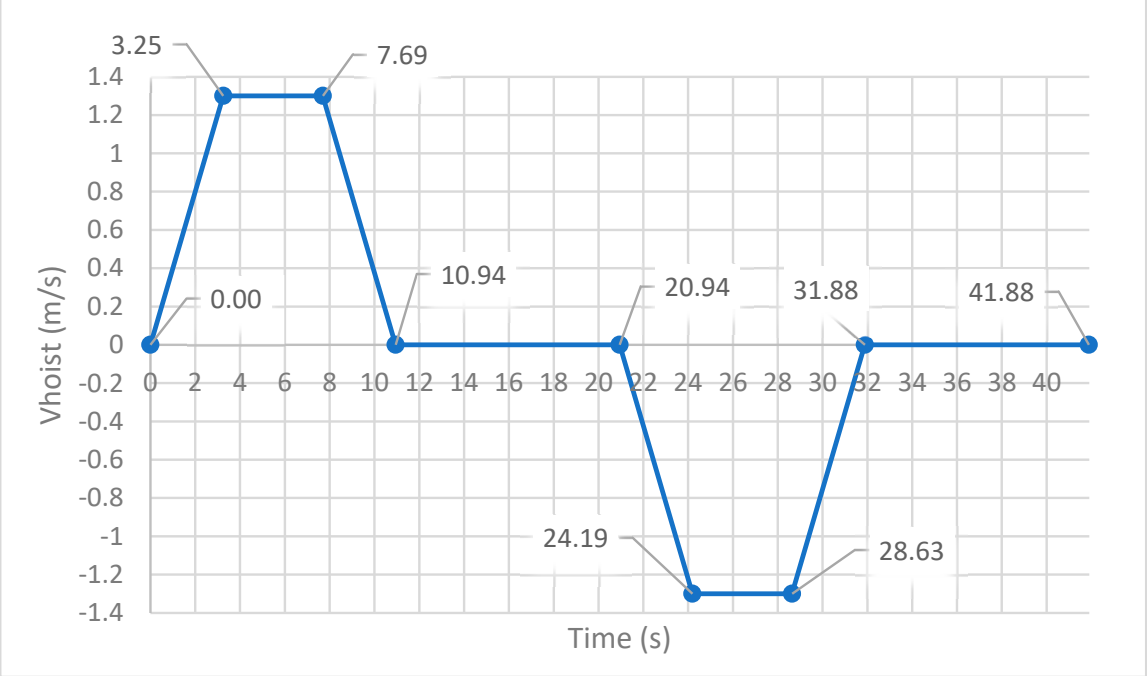

Figure 3. VTD carriage hoisting speed (m/s) versus time (s) chart.

The operating cycle steps are:

1—Upward movement of the hoisting carriage with load on the conveyor, Figure 2A. According to Figure 3, from 0 s up to 3.25 s, the hoisting carriage accelerates, reaching the speed of 1.3 m/s. Between 3.25 s and 7.69 s, the hoisting carriage will move upward at a constant speed, followed by a 3.25 s deceleration.

2—Transfer of the load from the conveyor mounted on the hoisting carriage, to the grounded conveyor on the upper level, Figure 2B. This transfer movement will take 10 s. During this time, the hoisting carriage is stopped.

3—Downward movement of the hosting carriage from the upper level to level 0, Figure 2B. This movement will start at 20.94 s and is composed of an acceleration of 3.25 s, followed by a constant speed movement of 4.44 s, and finally, a 3.25 s deceleration.

4—The load will be transferred from the grounded conveyor at level zero, to the conveyor mounted on the hoisting carriage, which is stopped. This transfer will take 10 s, Figure 2C.

Speeds and acceleration values in these machines are not prescribed. Instead, the design of the device, of its components and safety devices must be rooted in those values: the EN 619:2002+A1:2010 standard [14] does not define maximum speeds and accelerations for the VTD, but states that the safety related components must be selected according to the effective nominal speed and acceleration of the machine.

The upper sprocket assembly, which is the object of the present case study, is shown in Figure 4. It is composed of one shaft, two plummer blocks with roller bearings and one sprocket for the hoisting chain. Note that the failed shaft diameter was 50.0 mm.

Table 1. VTD upper drive assembly data before redesign.

Parameter	Value	Unit
v_{hoist} Hoisting carriage hoisting speed	1.3	m/s
a_{hoist} Hoisting carriage hoisting acceleration	0.4	m/s^2
D_p Sprocket pitch diameter	0.21304	m
a Position of the load on the shaft length	0.11	m
b Position of the load on the shaft length	0.11	m
d_i Initial shaft diameter, before redesign	0.05	m
c Initial sprocket length, before redesign	0.091	m
l Initial shaft length between supports	0.22	m
$m_{hoistcar}$ Hoisting carriage mass	600	kg
m_{load} Unit load mass	1600	kg
m_{lhd} Conveyor mass	350	kg
m_{count} Counterweight mass	1600	kg
m_{chain} Chain mass	300	kg
N Shaft rotating speed	12.15 (116)	rad/s (RPM)
η_l Load efficiency	0.9	

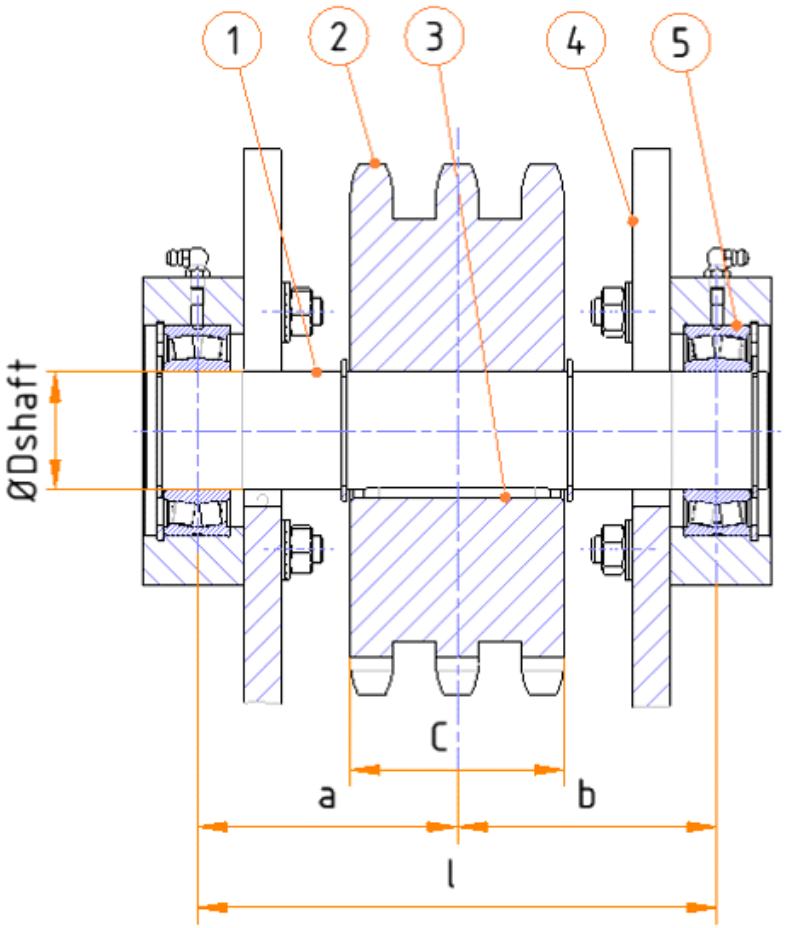

Figure 4. Components of the upper sprocket assembly: 1—upper sprocket shaft; 2—upper chain sprocket; 3—key; 4—upper sprocket assembly support; 5—roller bearings. See Table 1 for nomenclature.

The failure motivated the need for component redesign. As discussed in the following sections, a thorough understanding of the machine's operating mode is necessary for the selection of inputs to calculate the redesigned shaft diameter.

3. Assumptions for Calculation and Safety Factors

This section presents the selection of data to be used as inputs when calculating the shaft diameter and selecting the safety factors. Table 1 compiles the data for the case study system.

The load efficiency—η_l = 0.9—is the value advised by [15] for the efficiency of sprocket-chain hoisting systems, as some amount of the gearmotor output torque is not used to hoist the load, but to compensate friction losses, for instance.

The data for the gearmotor were retrieved from [15,16] and are compiled in Table 2.

Table 2. Gearmotor data for calculation; source: [16].

Parameter	Value	Unit
n_m Motor rotating speed	247.14 (2360)	rad/s (RPM)
J_M Motor moment of inertia	0.0381	kg·m^2
η_{motor} Motor efficiency	0.7833	-
i_t Total gearbox gear ratio	20.25	-
$\eta_{gearbox}$ Gearbox efficiency	0.96	-
a_{emerg} Gearmotor emergency deceleration, with brake	−4.829	m/s^2
M_{amax} Maximum nominal gearmotor torque	1500	N·m
M_{aemerg} Gearmotor torque in the event of an emergency deceleration with brake	1929	N·m

Unless there are problems associated with bearings, which is unlikely if these are properly selected and fitted according to the applicable tolerances, in these constructions, the likely cause of shaft failure is fatigue. Corrosion is excluded, given the shaft surface protection by phosphating surface treatment, and the machine's permanent location inside the warehouse.

A first check of the bearing life showed that the bearings were correctly chosen, and accordingly, bearing calculation and selection will be outside the scope of this paper. Since the failure was not related to the bearings, it was decided to further investigate the shaft design with a view to redesign. Given the level of responsibility involved, several calculation methods were used, and the results compared, to decrease the risk level.

Firstly, it was necessary to carefully define the assumptions for the calculation. The bending and torsion moments and the radial load to be considered for the design calculations were evaluated. Figures 5–7 present the evolution of these loads along the VTD operating cycle. For conciseness, the calculations behind Figures 5–7, based on [15,16], are not fully presented. Nevertheless, Section 5 includes the calculation of the maximum loads per operating cycle (i.e., the maximum values of the diagrams).

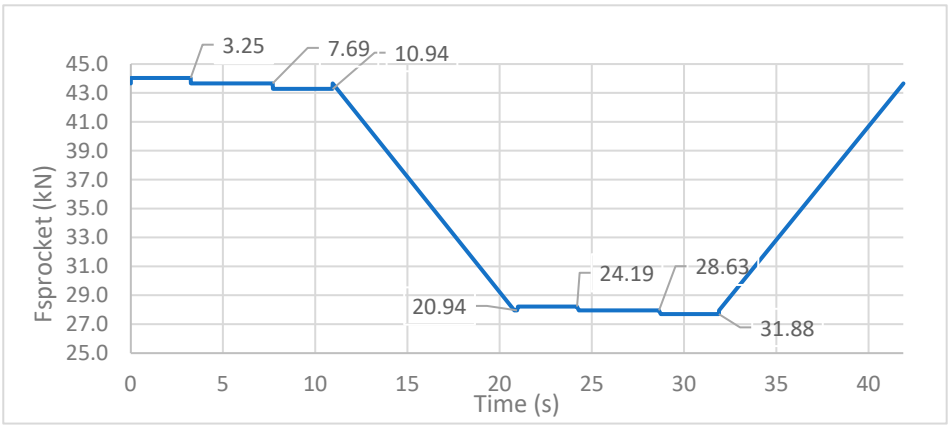

Figure 5. Radial load on the VTD upper sprocket (kN) vs. time (s).

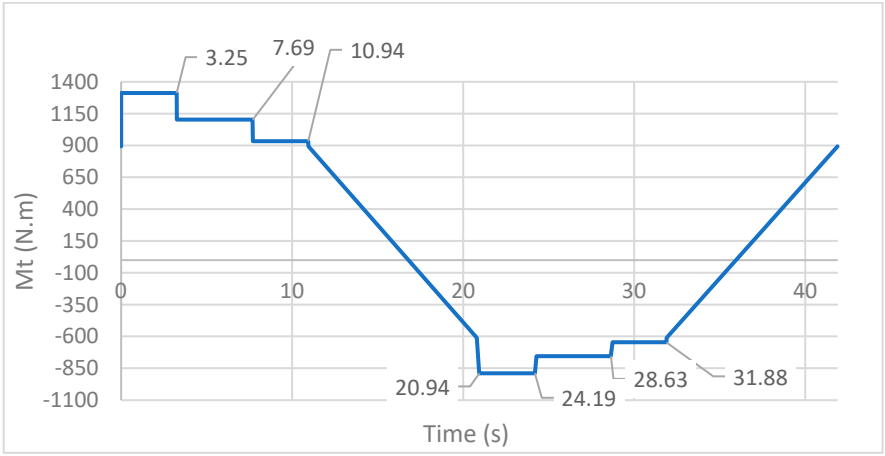

Figure 6. Torsional moment on the VTD hoisting shaft vs. time (s).

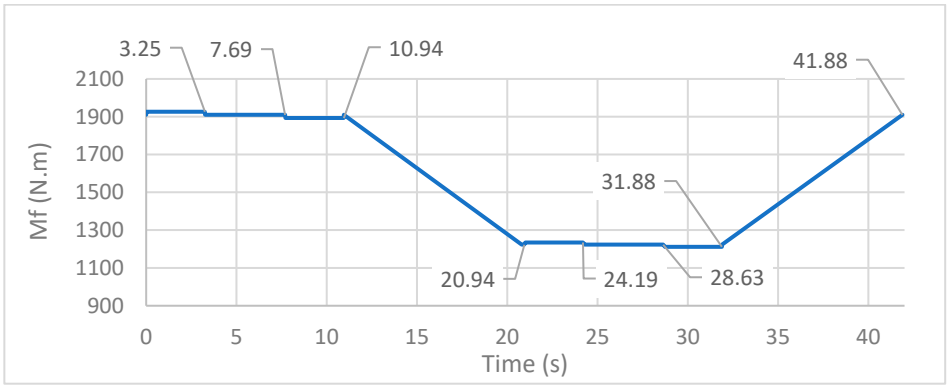

Figure 7. Bending moment on the VTD hoisting shaft vs. time (s).

The maximum vertical load on the sprocket, the maximum torsion moment and the maximum bending moment all occur when the hoisting carriage is accelerating upwards with its full maximum load. However, this only occurs between 0 and 3.25 s, i.e., in a small fraction of the machine's operating cycle, which takes nearly 41.9 s.

The total time with a full load on the hoisting carriage is about 50% of the overall working time. In the other 50%, the hoisting carriage is moving down without the unit load.

Shafts subjected to stresses below the yield strength but above the fatigue limit (also known as endurance strength) will most likely fail from fatigue. The fatigue limit is the operating stress at which the specimens do not fail after at least 10^6 cycles. Excluding consideration of giga-cycle fatigue, which is not relevant for this application, stresses below the fatigue limit lead to infinite life.

Milela [8] or Lee et al. [9] give overviews of a variety of fatigue topics; within that vast domain, this work concentrates on stress-based fatigue analysis and design for high-cycle fatigue (HCF), adopting the classical approach commonly used in industry. References such as [17,18] introduce classical fatigue design for HCF with a focus on machine elements.

It is crucial to understand which load values should be considered in the calculation methods described in Sections 6–8, and what the safety factors should be. Section 6 concerns the use of Niemann's approach [19,20], Section 7 concerns the use of the ANSI/ASME B106.1M:1985 standard [21], and a classical fatigue approach is used in Section 8. The methods considered give some guidance on these subjects but do not define them entirely.

Niemann, [19,20], introduces the safety factor C_v, and the overload factor C. To establish C_v, it is necessary to consider the consequences of overloads, e.g., danger of death,

long interruptions of the operation and production line or ease of repair or replacement of the damaged shaft. The overload factor C is defined as:

$$C = \frac{F_{serv}}{F} \quad (1)$$

where F_{serv} is the maximum load that occurs periodically in the machine cycle, and F is the nominal load.

The ANSI/ASME B106.1M:1985 standard [21] does not directly define the values for the safety factor (SF). Nevertheless, it states that SF should be considerably higher than 1 if there are great uncertainties and the consequences of failure are serious, namely, in terms of safety and production stopping time. The same standard also introduces the duty cycle factor k_e and states that a shaft usually withstands variable amplitude loadings in service. Thus, the shaft design must consider start and stop cycles, transient overloads, vibrations and shocks, since these transients can have a significant impact on fatigue life. Usually, the values for the constant amplitude loads are known with sufficient accuracy, but the data for transient loads are not so well defined. Nevertheless, in the present case study, it was possible to determine the transient loads that occur in the acceleration and deceleration phases of the VTD operating cycle. The ANSI/ASME B106.1M:1985 standard [21] states that it is not advisable to design a rotating shaft for finite fatigue life, as it will be confirmed in the following paragraphs.

An emergency stop will cause an overload on the hoisting shaft, and such events will certainly occur during the VTD service life. It is not possible to foresee how many times an emergency stop event will occur, but it will not be a very rare event. More unusual is the event of a free-fall with actuation of the safety gear. Overloads originated by the transfer of a load greater than the nominal maximum may also occur, but in this case, the hoisting carriage's vertical movement will not be initiated. The EN 619:2002 + A1:2010 [14] states that the system incorporating the VTD should prevent this from happening, for example, by assembling load cells on the conveyors that feed the VTD.

After analysing the inputs from these methods, some important decisions need to be made. If the nominal static load on the shaft is considered, an overload factor $C > 1$ should be selected. Another option is to use the dynamic load (including the VTD acceleration), and the overload factor C is taken as 1. Recall that according to Niemann [19], Equation (1), F_{serv} is a load that repeats periodically.

It was decided to use the loads that occur during the initial 3.25 s of the operating cycle, where the hoisting carriage is accelerating upwards, in all the fatigue calculation methods. It is important to maintain the consistency of the previous decision with the safety factors and coefficients that will be used in each of the formulations, to avoid over-design. As explained previously, within the operating cycle, the VTD is half of the time with load and half of the time without load, which has a beneficial effect on fatigue life.

In [2], Childs suggests the following safety factors for shaft design:

- "1.25 to 1.5 for reliable materials under controlled conditions subjected to loads and stresses known with certainty,
- 1.5 to 2.0 for well-known materials under reasonably constant environmental conditions subjected to known loads and stresses,
- 2.0 to 2.5 for average materials subjected to known loads and stresses,
- 2.5 to 3.0 for less well-known materials under average conditions of load, stress, and environment,
- 3.0 to 4.0 for untried materials under average conditions of load, stress, and environment, and
- 3.0 to 4.0 for well-known materials under uncertain conditions of load, stress, and environment".

The material used for the shaft under study is well known and reliable, and the environmental conditions are controlled and constant. The normal operation loads and the emergency stop loads are known, however, the number of occurrences of an emergency stop

is unclear. As mentioned previously, the present work will size the shaft for the maximum loads within the equipment operating cycle, which only occur during 3.25 s of the overall cycle time. This is a defensive approach; therefore, a small safety factor within the range was used—1.5. Another option might have been to consider the weighted average between the maximum loads that occur during the 50% of the time that the hoisting carriage is going upwards with maximum load and the 50% of the time that the hoisting carriage is moving downwards without load. If the last approach had been used, the safety factor would have been increased to 2.

The decision was to consider the loads occurring in the upward acceleration phase; therefore, $C = 1$, according to Niemann [19,20]. The safety factor was defined to be $C_v = 1.5$, instead of using higher safety factors, since the hoisting carriage is under load only half of the operating cycle time.

Likewise, in the ANSI/ASME B106.1M:1985 standard [21] method, the safety factor was defined as $SF = 1.5$, and the duty cycle factor was chosen to be $k_e = 1$.

The stress originated by the loads acting on the hoisting shaft must be classified. It is intuitive that the bending moment due to the radial load on the sprocket will cause an alternating stress on the rotating shaft. It is less intuitive how the torsional moment should be categorized. Niemann [20] defines a steady, an oscillating and an alternating stress. Notice that the direction of rotation of the hoisting shaft only reverses two times in each VTD operation cycle. Therefore, it would seem too defensive to consider the torsion as an alternating stress. At first sight, it would seem nearly steady. However, as discussed in the following paragraphs, the torsional load will cause an alternating stress that should be taken into account for infinite life calculation.

Another question that may arise is whether the infinite fatigue life design, corresponding to more than 10^6 cycles, is necessary. Would it be acceptable to calculate the shaft for a finite life, which would result in a smaller shaft diameter?

A shaft replacement is a complicated operation that may cause long production line downtime. Thus, it may be reasonable to require that the shaft not need to be replaced within the machine's lifespan. In this case study, 10 years were considered based on the assessment of the number of load cycles. In each complete rotation of the shaft, the hoisting carriage moves 0.67 m up. Since the VTD hoisting stroke is 10 m, the shaft will complete almost 15 rotations in the upward movement plus 15 complete rotations in the downward movement. In each 180 degrees of shaft rotation, there is one alternating bending cycle. So, 30 complete shaft rotations will correspond to 60 bending cycles. The throughput of the VTD is 85 pallets per hour, so the shaft will suffer 5134 bending cycles per hour. Since the VTDs will be operating in an automatic system that works 24 h a day, the shaft will withstand 123,186 bending cycles/day, 30,796,594 per year, and 308×10^6 cycles in 10 years. Thus, it is mandatory to calculate the shaft for infinite life. In the previous calculation, 250 working days per year were considered, according to DIN 15020:1974 [22].

Regarding the torsion stress, and applying the same rational, there will be 85 alternating torsional stress cycles per hour (two per machine up and down cycle), 4122 in each day, 1,030,585 per year and around 10×10^6 cycles in 10 years, much lower than the number of alternating stresses due to the rotational bending but still larger than the 10^6 cycles, which justify an infinite life calculation. Figure 8 shows schematically the relationship between both stresses. The graphic was simplified to allow better visualization, since 30 periods of the alternating bending stress curve would occur before the inversion of the signal of the alternating torsional load stress.

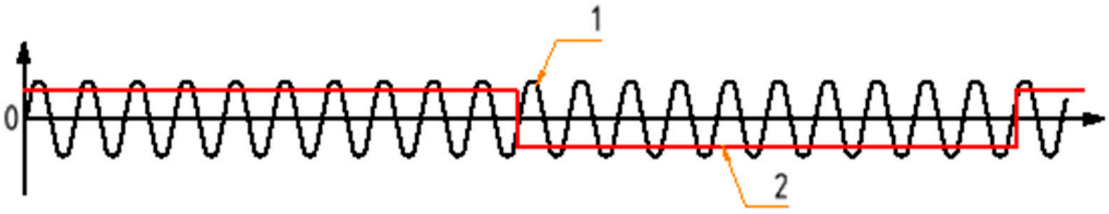

Figure 8. Schematic representation of bending and torsion stresses along the machine life. The discontinuity in the red line is a consequence of the torsion moment changing signal when the vertical movement is reversed: 1—Alternating bending stress: black line; 2—Alternating torsion stress: red line.

4. Shaft Diameter Calculation—Peak Loads

After the thorough analysis of the system and the definition of the input values for calculations, a first analysis concerns shaft behaviour under peak loads. The input data are found in Tables 1 and 2, including the parameters description. The notation for this and subsequent sections is given in Nomenclature part. The ANSI/ASME B106.1M:1985 standard [21] notes that there is not a comprehensive method to determine the impact of the peak load on the shaft fatigue life. Miner's law could be used if the occurrence of peaks could be quantified, but in the present case, the number of occurrences is unpredictable, precluding their explicit consideration in fatigue calculation.

The peak load to be considered results from the emergency stop by the gearmotor brake, which results in a torsional moment M_{aemerg} = 1929 N·m, and an acceleration of a_{emerg}= −4.829 m/s^2. The previous values were obtained using the software [16]; refer to Table 2. The radial load F_{peak}, acting on the hoisting shaft on an emergency gearmotor brake, is calculated as

$$F_{peak} = \left(m_{hoistcar} + m_{load} + m_{lhd}\right)\cdot\left(g - a_{emerg}\right) + m_{count}\cdot\left(g + a_{emerg}\right) + m_{chain}\cdot g \quad (2)$$

$$p_{peak} = \frac{F_{peak}}{c} \quad (3)$$

Figure 9 presents a model and the notation used. Recall that the failed shaft diameter was d_i = 50 mm.

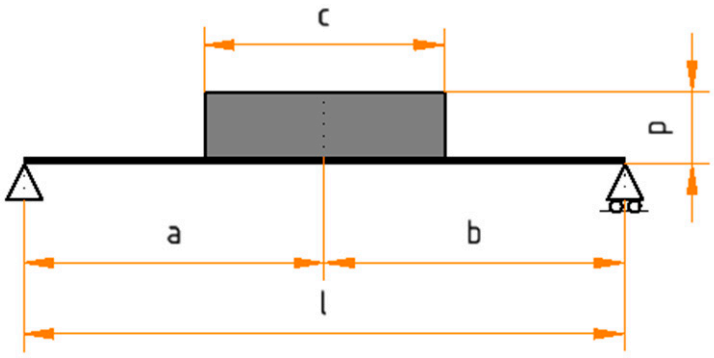

Figure 9. Load diagram.

In the shaft critical section and under the peak load, the bending moment and stress, the shear stress due to the load and to the torque, are calculated as:

$$M_{fpeak} = \frac{p_{peak}bc}{2l}\left(2a - c + \frac{bc}{l}\right) \quad (4)$$

$$I_{d_i} = \frac{\pi d_i^4}{64} \tag{5}$$

$$I_{p_{di}} = \frac{\pi d_i^4}{32} \tag{6}$$

From Equation (4), M_{fpeak} = 2092 N·m; from (5), $I_{D_2} = 3.07 \times 10^{-7}$ m^4; and from Equation (6), $I_{p_{di}} = 6.14 \times 10^{-7}$ m^4.

$$\sigma_{peakbending} = \frac{M_{fpeak}}{I_{d_i}} \cdot \frac{d_i}{2} \tag{7}$$

$$\tau_{peaktorsion} = \frac{M_{aemerg}}{I_{p_{di}}} \cdot \frac{d_i}{2} \tag{8}$$

$$\tau_{mpeak} = \frac{4}{3} \frac{V_{peak}}{A_{di}} \tag{9}$$

$$V_{peak} = \frac{p_{peak} bc}{l} - p \cdot \left(\frac{c}{2} - a + x \right), \; a = b = \frac{l}{2} \tag{10}$$

From Equation (7), $\sigma_{peakbending} = 170$ MPa; from Equation (8), $\tau_{peaktorsion} = 79$ MPa. Replacing $x = l/2$, in Equation (10), $V_{peak} = 0$ N, in the critical middle section of the keyseat area; thus, $\tau_{mpeak} = 0$ MPa, from Equation (9). The total shear stresses will be $\tau_{peak}^{eq} = 79 + 0 = 79$ MPa.

To conclude this static strength analysis, the von Mises criterion was used:

$$\sigma_{peak} = \sqrt{{\sigma_{peakbending}}^2 + 3 \cdot {\tau_{peak}^{eq}}^2} < \frac{\sigma_{yield}}{N_{peak}} \tag{11}$$

For steel 34CrNiMo6, refer to Table 3, and considering $N_{peak} = 1.5$, Equation (11) gives $\sigma_{peak} = 218$ MPa < 533 MPa, confirming that the shaft can withstand the peak load, and implying that its failure is likely due to fatigue. Unfortunately, the broken pieces were not available, so no scanning electron microscopy could be used to possibly identify striations. The work proceeded with a fatigue analysis using several methodologies.

Table 3. Comparison of the mechanical properties of the steels.

European Standard Designation	Tensile Strength σ_r for 40 < d < 100 mm	Yield Strength- $Rp_{0.2}$ for 40 < d < 100 mm
S355 Jr	500 MPa	325 MPa
34 CrNiMo 6 (1.6582)	1000 MPa	800 MPa

5. Calculation of the Normal Operation Loads on the Hoisting Shaft

According to Section 3, the acceleration loads will be considered for the fatigue calculation, and the safety factor will be adjusted to avoid overdesign. The input data are found in Tables 1 and 2, including the parameters description. The other notation is given in Nomenclature part. The gearmotor will transmit a torque to the bottom and upper sprocket to compensate the unbalance between the total maximum suspended mass—m_{tmsm}—and the counterweight mass. The chain does a closed loop, so the gearmotor torque does not need to take into account the chain weight; refer to Figure 1.

$$F_{unbalance} = (m_{tmsm} - m_{count}) \cdot g \tag{12}$$

$$M_{static} = \frac{F_{unbalance} \cdot \frac{D_p}{2}}{\eta_l} \quad (13)$$

From (12), the $F_{unbalance}$ = 9320 N, and from (13), the gearmotor static torque—M_{static} = 1103 N·m. M_{static} is the output torque required to the gearmotor to ensure the hoisting movement at constant speed. However, the load must be accelerated and decelerated within the operating cycle. Thus, the acceleration torque—M_H—takes into account the inertia of the moving bodies, including the gearmotor and motor inertias. The equations to calculate M_H are given in [15], and some data and inputs can be found by using the calculation software [16]. Table 2 presents input data for calculation.

$$J_x = 91.2 \cdot \frac{F_{unbalance}}{g} \cdot \left(\frac{v_{hoist}}{n_m}\right)^2 \quad (14)$$

$$M_L = \frac{F_{unbalance} \cdot v_{hoist} \cdot 9.55}{n_m} \quad (15)$$

$$M_H = \frac{\left(J_M + \frac{J_X}{\eta_{motor}}\right) \cdot n_m}{9.55 \cdot t_a} + \frac{M_L}{\eta_{motor}} \quad (16)$$

From (14), $J_x = 0.02629$ kg.m^2, and from (15), $M_L = 49$ N·m. Since v_{hoist} =1.4 m/s and $a_{hoist} = 0.3$ m/s^2, $t_a = 3.25$ s. With these values, from (16), the torque on the motor output shaft—M_H = 68 N·m. The torque in the gearmotor output shaft—M_{taccel} is calculated according to Equation (17).

$$M_{taccel} = M_H \cdot i_t \cdot \eta_{gearbox} \quad (17)$$

According to the input data from Table 2, the total gearbox transmission ratio $i_t = 20.25$, and the gearbox efficiency $\eta_{gearbox}$ = 96%, resulting in a M_{taccel} = 1323 N·m.

The radial load on the sprocket during the upward accelerating movement of the hoisting carriage with maximum load—F_{accel}—is calculated according to (18), and the bending moment is calculated by using the Equations (19) and (20), resulting in F_{accel} = 44035 N and M_{faccel} = 1927 N·m.

$$F_{accel} = (m_{hoistcar} + m_{load} + m_{lhd}) \cdot (g + a_{hoist}) + m_{count} \cdot (g - a_{hoist}) + m_{chain} \cdot g \quad (18)$$

$$p_{accel} = \frac{F_{accel}}{c} \quad (19)$$

$$M_{faccel} = \frac{p_{accel} bc}{2l}\left(2a - c + \frac{bc}{l}\right) \quad (20)$$

6. Calculation of the Shaft Diameter According to the Niemann Method

After defining the load values to be used as input for all the shaft diameter calculation methods (refer to Section 5), the first calculation was done according to Niemann [19] (see Table 17.2 of that reference). For a torsional load M_{taccel}= 1323 N·m, it defines a shaft diameter of around 80 mm, whereas before the present redesign, the diameter was only 50 mm. Even if the reference used (Table 17.2 of [19]) considers a lower strength steel, as will be seen later, this first calculation showed that the shaft design required attention.

Still in [19], a more detailed calculation method may be found (Table 17.5 of that reference). For a shaft under torsional and bending loads, Equations (21) and (22) are introduced.

$$M_{eq} = \sqrt{{M_f}^2 + \left(\frac{a_f}{2} M_t^2\right)} \quad (21)$$

$$d_N = 2.17 \cdot \sqrt[3]{\frac{M_{eq}}{\sigma_f} b_N} \tag{22}$$

For a solid shaft, $b_N = 1$, a_f= 1 for oscillating torsion with alternate bending, and $a_f = 1.7$ for alternating torsion and bending. As shown in Section 3, and contrary to how it may seem at first sight, the torsional load is also to be considered alternating.

The Niemann method defines a σ_{fad} = 500 kgf/cm^2 (~50 MPa), for ST50.11 steel on a hoisting shaft application. The mechanical properties of the ST50 steel could be considered equivalent to the current steel S355 Jr of NP EN 10025 + A1:1994 [23]. Currently, higher strength steels are used in this type of application. Table 3 compares the mechanical properties of the S355 Jr steel (NP EN 10025 + A1:1994, [23]) with the 34CrNiMo6 steel (EN 10083:2006 [24]).

On first thought, the fatigue strength—σ_f—in a keyway torque transmission area of a 34CrNiMo6 shaft might be expected to be approximately twice that of a ST50 one. However, as shown in Niemann [20], the use of high strength steels does not improve so much the allowable fatigue stress for a shaft under alternating bending in a keyway area—σ_{fa10}. In [20] (Figure 3.27 of that ref.), σ_{fa10} is 105 MPa for the ST50 steel, and increases to around 120 MPa for a steel with σ_r = 800 MPa, the highest value considered. Extrapolating, see the blue dotted line in Figure 10, σ_r = 1000 MPa corresponds to σ_{fa10} = 125 MPa. Notice that σ_{fa10} is the allowable fatigue strength in keyway under alternating bending for one test specimen with a diameter of 10 mm and a material with a given σ_r.

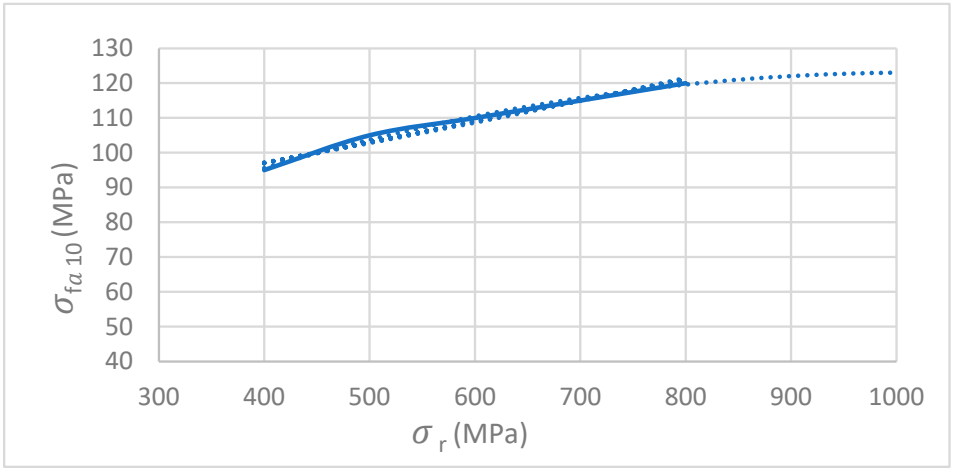

Figure 10. Allowable fatigue strength in a keyseat area σ_{fa10}, for steels with tensile strength σ_r.

To calculate the allowable fatigue strength in the critical area of the shaft, the keyway area, it is necessary to consider other factors according to:

$$\sigma_{fa} = \frac{\sigma_{fa10} . b_0}{C_v . C} \tag{23}$$

Considering the shaft diameter of 50 mm, the size factor is $b_0 = 0.7$; refer to Table 4. According to Section 3, the safety factor C_v is 1.5, and the overload factor $C = 1$. From (23), σ_{fa} = 58 MPa in the keyseat area.

Table 4. Size factor for different shaft diameters according to [20].

Shaft diameter—d_{shaft}	10	20	30	50	100
Size factor b_0	1	0.9	0.8	0.7	0.6

The results from the calculation with Equations (21) and (22) are summarized in Table 5. The first iteration resulted in a shaft diameter of 73 mm, so the b_0 value was corrected to 0.65 in the second iteration. According to [20], for oscillating torsion with alternate bending, the diameter of the shaft in the keyway area would need to be 72.5 mm considering a_f = 1, and 74.8 considering a_f = 1.7 for alternating torsion and bending. Recall that before the redesign, the shaft diameter was 50 mm only, so it looked unsatisfactory. Even considering $C_v = 1$, $C = 1$ and a_f = 1, the required shaft diameter would need to be higher than 50 mm, around 63 mm.

Table 5. Results from the application of Niemann's method, [20].

	Equivalent Moment M_{eq}	**Resulting Shaft Diameter** d_N
Alternating bending and oscillating torsion a_f = 1	2037 N·m	72.5 mm
Alternating bending and torsion $a_f = 1.7$	2230 N·m	74.8 mm

As already explained, the input values in the previous calculation were $M_f = M_{faccel} = 1927$ N·m and $M_t = M_{taccel}$ = 1323 N·m.

7. Calculation of the Shaft Diameter According to ANSI/ASME Methodology

Given the losses incurred with the failure, and since the redesigned shaft is intended for use in several future machines, it was decided, for comparison purposes, to use yet another procedure to redesign the shaft for infinite life, following the ANSI/ASME B106.1M:1985 standard, [21]. Although now withdrawn, this standard is a commonly used guide for shaft design, as stated, e.g., by Childs, [2,3], and it continues to be included in ANSI/CEMA B105.1-2015, [25]. The notation from the standard [21] is used here.

According to [21], for steels with ultimate tensile strengths lower than 1400 MPa, such as the 34CrNiMo6 steel, in the absence of detailed testing, the approximation $S_f{}^* = 0.5S_u$, where $S_f{}^*$ is the fatigue limit of polished unnotched test specimen in reversed bending, and S_u is the ultimate tensile strength of the steel, should provide reasonable accuracy.

According to ANSI/ASME B106.1M:1985, [21], the shaft diameter is calculated using Equation (24) based upon the von Mises criterion,

$$d = \left(\frac{32FS}{\pi}\right)^{\frac{1}{3}} \left[\sqrt{\left(\frac{M_f}{S_f}\right)^2 + \frac{3}{4}\left(\frac{T}{S_y}\right)^2}\right]^{\frac{1}{3}} \quad (24)$$

where d is the shaft diameter (m), FS is the factor of safety and S_f is the corrected endurance (fatigue) limit of the shaft in reversed bending, calculated using Equation (25), S_y is the tensile yield strength (N/m^2) of the steel, T is the static mean torque (N·m) and M_f is the reverse bending moment (N·m). Using Tresca instead of von Mises, this classical result is found, e.g., in [26] (chapter 13).

The following Equation (25) from [21] is also presented in many publications. Given its important role in the present analysis, its use is presented in some detail in the following paragraphs.

$$S_f = k_a k_b k_c k_d k_f k_e k_g S_f{}^* \quad (25)$$

The first correction factor in Equation (25) is the surface finish factor k_a. This factor accounts for the difference in the surface condition between the shaft under evaluation and one highly polished test specimen. As recalled in the ANSI/ASME standard, experiments have shown that the surface condition can have an important effect on the fatigue strength, since fatigue cracks are usually initiated at the surface of the shaft, where stresses are higher. For reference, the machined surface category is to be considered for shafts with surface roughness ranging from Ra 1.6 to Ra 6.3 μm.

According to [21], for the shaft under evaluation with Ra 3.2 µm, manufactured in 34CrNiMo6, with ultimate tensile strength S_u = 1000 MPa, $k_a = 0.72$, Figure 11.

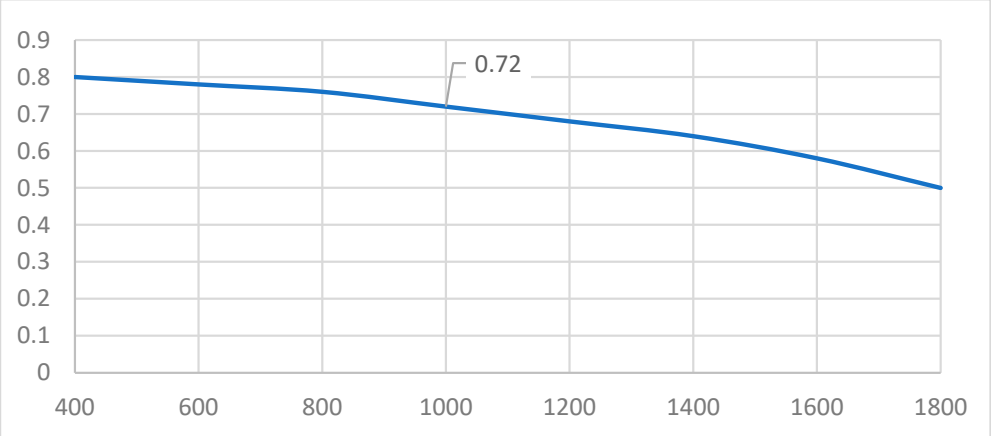

Figure 11. Surface finish factor—k_a—for a machined shaft, according to [21].

The size factor k_b quantifies the decrease of the fatigue limit with the increase of the diameter, as briefly discussed in [21], where different equations for k_b depending on the diameter range, are presented. For shafts with a diameter larger than 50 mm and lower than 254 mm, Equation (26) is to be used; thus, for the case study diameter of 50 mm, $k_b = 0.88$.

$$k_b = 1.85d^{-0.19} \tag{26}$$

According to [21], the reliability factor k_c should be taken in account, due to the variability of the mechanical properties of the specimen. In a safety risk assessment analysis, the VTD hoisting shaft would be considered critical, as its rupture would allow the hoisting carriage to free fall. The factor k_c reduces the fatigue limit, so that a smaller percentage of the population fails during the machine's life, increasing reliability. In this calculation, a reliability rate of 90% was chosen, so k_c = 0.897; refer to Table 6.

Table 6. Reliability factors k_c according to [21].

Shaft Nominal Reliability	k_c
0.5	1
0.9	0.897
0.99	0.814

The temperature factor k_d, translates the effect of the temperature on the fatigue limit. There is a trend to use VTDs in cold temperatures, down to −30 °C in deep freeze warehouses, so this factor appeared to be relevant. The ANSI/ASME standard states that for operating temperatures from −57° to 204°, the fatigue limit is not affected by temperature for most steels, so $k_d = 1$.

The duty cycle factor—k_e—was already discussed in Section 3. The value $k_e = 1$ will be considered for this calculation (refer to Section 3 for more details).

The miscellaneous effects factor—k_g—concerns different factors that may affect the fatigue life (e.g., residual stresses from the manufacturing process, corrosion, surface coating). Its value was taken as $k_g = 1$, addressing this uncertainty with the safety factor.

Failure usually occurs in a notch, keyway, shoulder or other discontinuity where the stresses are amplified. The fatigue stress concentration factor—k_f—represents the effect of the stress concentration on the fatigue limit of the shaft, according to Equation (27).

$$k_f = \frac{fatigue\ limit\ of\ the\ notched\ specimen}{fatigue\ limit\ of\ a\ specimen\ free\ of\ notches} = \frac{1}{K_f} \tag{27}$$

where K_f is the fatigue strength reduction factor and is calculated according to Equation (28). Equations (27) and (28) are used by the ANSI/ASME B106.1M:1985 standard [21], found in many references that address the fatigue damage mechanism, such as [11,18], for instance.

$$K_f = 1 + q(K_t - 1) \tag{28}$$

where q is the notch sensitivity of a given material. The notch sensitivity can be used to relate the fatigue strength reduction factor—K_f—to the theoretical stress concentration factor K_t. It is interesting to know that experience has shown that low-strength steels are less sensitive to fatigue at notches than the high-strength steels. For more details, refer to [18] (Section 1.9). Ref. [21] gives directly the value for k_f for a profiled keyway under bending stress in solid round steel shafts, according to Table 7, without the need to determine the notch sensitivity factor q, nor the theoretical stress concentration factor K_t.

Table 7. Fatigue stress concentration factor k_f, for a profiled keyway under bending stress in solid round steel shafts, according to [21].

Steel	k_f
Annealed (less than 200 BHN [27])	0.63
Quenched or drawn (more than 200 BHN [27])	0.5

The shaft material—steel 34CrNiMo6, EN 10083-3:2006 [24], has a Brinell hardness number—BHN [27]—higher than 200, so $k_f = 0.5$.

By entering all the values for the factors in Equation (25), S_f = 142 MPa. From Equation (24), considering FS = 1.5, the minimum shaft diameter would be 59.3 mm. This shows that the 50 mm diameter is not enough to ensure the fatigue strength of the shaft.

As already explained, the input values in the previous calculation were $M_f = M_{faccel} = 1927$ N·m, and $T = M_{taccel} = 1323$ N·m.

The ANSI/ASME standard considers reversed bending and steady or nearly steady torsion. However, as seen in Section 3, in the present case, the torsion is also alternating, albeit with a lower frequency. Although the number of reversed torsion cycles is much lower than the number of reversed bending cycles, it will surpass 10^6 cycles and should be considered in the shaft design. These circumstances led to a final fatigue calculation that could fully accommodate the service conditions of the shaft, as presented in the next section (Section 8).

8. Calculation of the Shaft Diameter Taking into Account the Alternating Torsion

The ANSI/ASME B106.1M:1985 standard [21] is based on classical fatigue design considerations. It represents a particular situation of a more general treatment presented, e.g., in [26], or in [4,5,28], and other references mentioned in Section 1. In the following, the notation of [17] is adopted.

Refs. [17,21] define the fatigue limit strength—S'_n—as $S'_n = 0.5S_u$, where S_u is the ultimate tensile strength, and it is necessary to affect the fatigue limit strength with the correction factors. Table 8 defines the load type factor C_L.

Table 8. Fatigue strength correction factors C_L for each type of loading, according to [17].

	Load Type		
Fatigue Strength Correction Factor—Load Factor	**Axial**	**Bending**	**Torsion**
C_L	0.85	1	0.58

The gradient factor, also known as size factor C_G, is equivalent to the ANSI/ASME method factor k_b and is shown in Table 9.

Table 9. Gradient correction factors C_G for each type of loading, according to [17].

Fatigue Strength Correction Factor—Gradient Factor	Load Type		
	Axial	**Bending**	**Torsion**
C_G for $10 < d_{shaft} < 50$	0.7 to 0.9	0.9	0.9
C_G for $50 < d_{shaft} < 100$	0.6 to 0.8	0.8	0.8

The surface finish factor C_S, is equivalent to the ANSI/ASME method factor k_a. According to [17], $C_S = 0.72$, the same as k_a. The temperature factor is $C_T = 1$ for the case study appliance environmental temperatures.

Similar to the ANSI/ASME method, the reference [17] introduces the reliability factor C_R, with the same values shown on Table 6 of Section 7. Thus, $C_R = 0.897$.

So, the limit fatigue strength will be corrected by these factors according to Equation (29) for the rotating bending stress, and (30) for the alternate torsional load.

$$S_{nb} = S'_n C_{Lb} C_G C_S C_T C_R \tag{29}$$

$$S_{nt} = S'_n C_{Lt} C_G C_S C_T C_R \tag{30}$$

resulting in $S_{nb} = 258$ MPa for the rotational bending load, and $S_{nt} = 150$ MPa for the reversed torsional load.

As in the ANSI/ASME method, ref. [17] gives directly K_f for profiled keyways, according to Table 10.

Table 10. Fatigue stress concentration factor k_f, for a profiled keyway under bending stress in solid round steel shafts, according to [17].

Steel	Bending	Torsion
	K_{fb}	K_{ft}
Annealed (less than 200 BHN [27])	1.6	1.3
Quenched or drawn (more than 200 BHN [27])	2.0	1.6

As explained in Section 7, BHN is larger than 200, so $k_{fb} = 2$ and $k_{ft} = 1.6$.

In the previous table, it is possible to notice the fundamental tendency for the harder and stronger materials to be more notch-sensitive. This means that changing from a soft to a harder and stronger steel normally increases part fatigue strength, but the increase is not as great as might be expected because of the increased notch sensitivity. As can be seen in Table 10, the harder material with 200 BHN has a stress concentration factor—K_f—greater than the softer material.

There are different types of loads acting on the keyway area—bending and shear stress due to the radial load on the sprocket, torsional load due to the gearmotor output torque. Equivalent stresses σ^{eq} were calculated as

$$\sigma^{eq} = \sigma_m + \frac{S_y}{S'_n C_{Lb} C_G C_S C_T C_R} K_{fb} \sigma_{abending} \tag{31}$$

$$\tau^{eq} = \tau_m + \frac{\frac{S_y}{\sqrt{3}}}{S'_n C_{Lt} C_G C_S C_T C_R} K_{ft} \tau_{atorsion} \tag{32}$$

where σ_m and τ_m are the mean stresses. The bending stress has zero mean stress, $\sigma_m = 0$ (or $R = \sigma_{min}/\sigma_{max} = -1$). The alternate bending stress—$\sigma_{abending}$—results from the bending moment calculated in Section 5—$M_{faccel} = 1927$ N·m, and the shear stress—$\tau_{atorsion}$—

results from the alternating torsional load calculated in Section 5 M_{taccel} = 1323 N·m.

$$\sigma_{abending} = \frac{M_{faccel}}{I_{d_i}} \cdot \frac{d_i}{2} \tag{33}$$

$$\tau_{atorsion} = \frac{M_{taccel}}{I_{p_{di}}} \cdot \frac{d_i}{2} \tag{34}$$

$$\tau_m = \frac{4}{3} \frac{V_{accel}}{A_{di}} \tag{35}$$

Considering a shaft diameter of 50 mm, as in the design before the redesign, using Equations (5) and (6), $I_{d_i} = 3.07 \times 10^{-7}\text{m}^4$, and $I_{p_{di}} = 6.14 \times 10^{-7}\text{m}^4$.

From Equation (33), $\sigma_{abending}$ = 157 MPa, and from (31), σ^{eq} = 972 MPa for the bending stress. For the torsional and shear stresses, from (35), τ_m = 0 MPa. As seen in Section 4, V_{accel} = 0 N in the middle section of the shaft—$\frac{l}{2}$—that is the critical section for fatigue calculation. From (34), $\tau_{atorsion}$ = 54 MPa, and (35), τ^{eq} = 266 MPa.

The final validation was done by applying the Tresca criterion according to Equation (36). In the context of classical fatigue design, the use of Tresca criterion is found, e.g., in [11].

$$\tau_{mx} = \sqrt{\left(\frac{\sigma^{eq}}{2}\right)^2 + \tau^{eq2}} < \frac{S_y}{2N_s} \tag{36}$$

where N_s is the safety factor.

For a shaft diameter of 50 mm, we have from Equation (36), τ_{mx} = 554 MPa, higher than the allowed 400 MPa, for N_s = 1; thus, far from ensuring infinite fatigue life!

It would be necessary to increase the shaft diameter to 63.9 mm to ensure infinite fatigue life, taking into account the alternating rotational bending load and alternating torsional load, with a safety factor of 1.5. Recall that this value is higher than the 59.3 mm that resulted from the ANSI/ASME method, Section 7, that did not take alternate torsion into account.

9. Conclusions

A redesign of a failed 50 mm diameter hoisting shaft was presented. The importance of making a thorough assessment of the VTD operation before the shaft redesign was emphasized, making it possible to realize that the torsional load from the gearmotor output torque should be considered alternating and taken into account as such in the fatigue redesign performed.

The peak load σ_{peak} = 218 MPa was seemingly low when compared with the fatigue limit σ_{f0} = 500 MPa (34CrNiMo6 steel). This might lead to the misleading consideration that the calculation of the shaft for fatigue was unnecessary, but that would be an expensive mistake.

In fact, the keyseat area is subjected to high stress concentration, with a serious impact on the maximum fatigue allowable stress. All the methods described in the present work indicate that the fatigue limit allowable stress in keyseat areas does not increase proportionally with the ultimate strength of the steel. This means that changing from a soft to a harder and stronger steel normally increases the part fatigue strength, but the increase is not as great as might be expected.

For the shaft material, according to a rough sizing presented by Niemann, the maximum allowable stress for infinite fatigue life in the keyseat area was 58 MPa, whereas it was 142 MPa according to ANSI/ASME, illustrating the conservativeness of the Niemann method.

The ANSI/ASME method was developed for steady torsional loads. To consider reversed torsional loading and ensure infinite fatigue life under reversed torsion and rotational bending, a classical fatigue model combining shear and torsional stresses with bending and normal stresses using equivalent stresses was performed.

Overloads, including possible misuses of the VTD, are difficult to quantify. According to ANSI/ASME and to Niemann, these transient loads need to be considered through the incorporation of safety factors that take into account the severity of a hoisting shaft rupture in terms of safety, machine damage and machine downtime.

The redesigned shaft diameter was, according to Niemann, d = 74.8 mm; according to the ANSI/ASME method, it was d = 59.3 mm; and according to the classical fatigue model, it would be d = 63.9 mm. Taking into account the transient overloads, finally, d = 70 mm was adopted for the redesigned shaft.

Author Contributions: Conceptualization, F.A.C.d.S. and P.M.S.T.d.C.; methodology, F.A.C.d.S.; investigation, F.A.C.d.S.; resources, F.A.C.d.S.; data curation, F.A.C.d.S.; writing—original draft preparation, F.A.C.d.S.; writing—review and editing, F.A.C.d.S. and P.M.S.T.d.C.; visualization, F.A.C.d.S. and P.M.S.T.d.C.; supervision, F.A.C.d.S.; project administration, F.A.C.d.S. All authors have read and agreed to the published version of the manuscript.

Funding: This research received no external funding.

Institutional Review Board Statement: Not applicable.

Informed Consent Statement: Not applicable.

Data Availability Statement: The data used in the work are presented in the text.

Acknowledgments: F.A.C.d.S. gratefully acknowledges Instituto Superior de Engenharia do Porto—ISEP, specifically, for access to technical literature relevant for researching the subject.

Conflicts of Interest: The authors declare no conflict of interest.

Nomenclature

Section 4		
A_{di}	Section area of the shaft with initial diameter	m^2
F_{peak}	Peak load on the hoisting shaft sprocket in a emergency stop	N
I_{di}	Inertia of the initial shaft diameter section	m^4
$I_{p_{di}}$	Polar inertia of the initial shaft diameter section	m^4
M_{fpeak}	Bending moment caused by the emergency stop radial load on the sprocket	N·m
M_{aemerg}	Peak emergency torque	N·m
N_{peak}	Safety factor for peak load stresses validation	---
p_{peak}	Distributed emergency radial load on the sprocket length	N/m
V_{peak}	Peak shear load on shaft, on $l/2$	N
σ_{peak}	Von Mises peak stress originated in emergency stop	MPa
$\sigma_{peakbending}$	Bending stress caused by the peak emergency radial load on the shaft critical section	MPa
σ_{yield}	Steel yield stress	MPa
τ_{mpeak}	Shear stress caused by the emergency stop radial load	MPa
τ^{eq}_{peak}	Equivalent shear stress originated in emergency stop	MPa
$\tau_{peaktorsion}$	Torsion stress caused by the peak emergency torque	MPa
Section 5		
F_{accel}	Load on the sprocket during the VTD acceleration and deceleration	N
$F_{unbalance}$	Load caused by the unbalance between m_{tmsm} and the counterweight mass	N
J_x	External moment of inertia reduced to the motor shaft	$kg.m^2$
M_{faccel}	Bending moment during VTD acceleration and deceleration	N

M_H	Acceleration torque	N·m
M_L	Load torque	N·m
M_{static}	Required gearmotor torque necessary to ensure the hoisting movement at constant speed	N·m
M_{taccel}	Output gearmotor torque during acceleration	N·m
p_{accel}	Distributed load on the sprocket during acceleration and deceleration	N
t_a	Acceleration time	s
m_{tmsm}	Total maximum suspended mass	kg
V_{accel}	Shear load on the shaft critical section equal to $\frac{F_{accel}}{2}$	N
η_{motor}	Motor efficiency	---
Section 6		
a_f	Factor for oscillating bending and alternating bending according to the Niemann method [20].	---
b_0	Size factor according to the Niemann method [20].	---
b_N	Factor for solid shafts or hollow shafts according to the Niemann method [20].	---
d_N	Resulting shaft diameter according to the Niemann method [20].	mm
M_{eq}	Equivalent moment for calculation of the shaft diameter according to the Niemann method [20].	N·m
M_f	Bending moment for calculation of the shaft diameter according to the Niemann method [20].	N·m
M_t	Torsion moment for calculation of the shaft diameter according to the Niemann method [20].	N·m
σ_{fa10}	Allowable fatigue strength in keyway under alternating bending for the test specimen with diameter 10 mm and a material with a given σ_r	---
σ_{fad}	Allowable fatigue strength in keyway under alternating bending for a given shaft diameter	MPa
σ_r	Ultimate tensile strength of the shaft steel	MPa
Section 7		
FS	Factor of safety according to ANSI/ASME [21]	---
K_f	Fatigue strength reduction factor according to ANSI/ASME [21]	---
K_t	Theorical stress concentration factor in bending according to ANSI/ASME [21]	---
k_a	Surface finish factor according to ANSI/ASME [21]	---
k_b	Size factor according to ANSI/ASME [21]	---
k_c	Reliability factor according to ANSI/ASME [21]	---
k_d	Temperature factor according to ANSI/ASME [21]	---
k_f	Fatigue stress concentration factor in a keyseat area under reversed bending according to ANSI/ASME [21]	---
$k_{ftorsion}$	Fatigue stress concentration factor in a keyseat area under reversed torsion according to ANSI/ASME [21]	---
k_g	Miscellaneous effects factor according to ANSI/ASME [21]	---
q	Notch sensitivity factor	---
S_f	Corrected fatigue limit of the shaft in reversed bending according to ANSI/ASME [21]	N/m^2
S_f^*	Fatigue limit of polished, unnotched test specimen in reverse bending according to ANSI/ASME [21]	N/m^2
S_{fa}	Allowable corrected fatigue limit of shaft in reversed bending according to ANSI/ASME [21]	N/m^2
S_u	Ultimate tensile strength of the shaft steel	N/m^2
S_y	Tensile yield strength of the steel	N/m^2
$S_{yctorsion}$	Allowable corrected fatigue limit of shaft in reversed (alternating) torsion	N/m^2
T	Static mean torque	N·m

Section 8		
C_G	Gradient factor	---
C_L	Load type factor	---
C_{Lb}	Load type factor for reversed bending	---
C_{Lt}	Load type factor for reversed torsion	---
C_R	Reliability factor	---
C_S	Surface finish factor	---
K_{fb}	Stress concentration factor in a keyseat area of a shaft in reversed bending	---
K_{ft}	Stress concentration factor in a keyseat area of a shaft in reversed (alternating) torsion	---
N_s	Safety factor for the conventional classical fatigue model calculation	---
S'_n	Fatigue limit strength of the steel	MPa
S_{nb}	Allowable corrected fatigue limit of shaft in reversed bending according to the conventional classical fatigue model	MPa
S_{nt}	Allowable corrected fatigue limit of shaft in reversed torsion according to the conventional classical fatigue model	MPa
S_u	Ultimate tensile strength of the steel	MPa
S_y	Tensile yield strength of the steel	MPa
$\sigma_{abending}$	Alternating bending stress	MPa
$\tau_{atorsion}$	Alternating torsion stress	MPa
σ_m	Mean normal stress	MPa
σ^{eq}	Equivalent normal stress, resulting from bending and traction loads combination	MPa
τ_m	Mean shear stress	MPa
τ^{eq}	Equivalent shear stress, resulting from torsion and shear loads combination	MPa

References

1. Harris, D.; Jur, T. Classical fatigue design techniques as a failure analysis tool. *J. Fail. Anal. Prev.* **2009**, *9*, 81–87. [CrossRef]
2. Childs, P.R.N. *Mechanical Design Engineering Handbook*, 2nd ed.; Elsevier/Butterworth-Heinemann: Oxford, UK, 2019.
3. Childs, P.R.N. *Mechanical Design: Theory and Applications*, 3rd ed.; Elsevier/Butterworth-Heinemann: Oxford, UK, 2021.
4. Beswarick, W.J. *Shaft with Fluctuating Loads. SEED—Sharing Experience in Engineering Design*; Engineering Design Procedural Guide; SEED: Hatfield, UK, 1988; guide MPT 6.2.
5. Beswarick, W.J. Shaft with fluctuating load. In *Rotary Power Transmission Design*; Hurst, K., Ed.; McGraw Hill: London, UK, 1994; pp. 142–148.
6. D'Angelo, A. *Machine Design for Technology Students. A Systems Engineering Approach*; Springer Nature: Cham, Switzerland, 2021. [CrossRef]
7. de Castro, P.M.S.T.; Fernandes, A.A. Methodologies for failure analysis: A critical survey. *Mater. Des.* **2004**, *25*, 117–123. [CrossRef]
8. Milella, P.P. *Fatigue and Corrosion in Metals*; Springer: Milan, Italy, 2013.
9. Lee, Y.L.; Pan, J.; Hathaway, R.; Barkey, M. *Fatigue Testing and Analysis. Theory and Practice*; Elsevier Butterworth–Heinemann: Oxford, UK, 2005.
10. Anes, V.; de Freitas, M.; Reis, L. The damage scale concept and the critical plane approach. *Fatigue Fract. Eng. Mater. Struct.* **2017**, *40*, 1240–1250. [CrossRef]
11. d'Isa, F.A. *Mechanics of Metals*; Addison-Wesley: Reading, MA, USA, 1968.
12. Hall, A.S.; Holowenko, A.R.; Laughlin, H.G. *Theory and Problems of Machine Design*; McGraw-Hill: New York, NY, USA, 1961.
13. Spotts, M.F. *Design of Machine Elements*, 3rd ed.; Prentice-Hall: Englewood Cliffs, NJ, USA, 1962.
14. *EN 619:2002+A1:2010*; Continuous Handling Equipment and Systems—Safety and EMC Requirements for Equipment for Mechanical Handling of Unit Loads. European Committee for Standardization: Brussels, Belgium, 2010.
15. SEW EURODRIVE. *Project Planning of Drives—Edition 10/2001*; SEW EURODRIVE: Bruchsal, Germany, 2001.
16. SEW EURODRIVE. SEW Workbench. Available online: https://www.sew-eurodrive.pt/servicos/engenharia_selecao/ferramentas_de_engenharia/ferramentas_de_engenharia.html (accessed on 4 March 2023).
17. Juvinall, R.C.; Marshek, K.M. *Fundamentals of Machine Component Design*, 6th ed.; John Wiley & Sons: Hoboken NJ, USA, 2017.
18. Pilkey, W.D.; Pilkey, D.F. *Peterson's Stress Concentration Factors*, 3rd ed.; John Wiley & Sons: Hoboken, NJ, USA, 2008.
19. Niemann, G. *Elementos de Máquinas*, 7th printing; Editora Edgard Blücher Ltda: São Paulo, Brazil, 2004; Volume II.
20. Niemann, G. *Tratado Teórico-Práctico de Elementos de Máquinas—Cálculo, Diseño e Construcción*, 2nd ed.; Editorial Labor, S.A.: Barcelona, Spain, 1973.
21. *ANSI/ASME B106.1M:1985*; Design of Transmission Shafting. ANSI/ASME: Washington, DC, USA, 1985.

22. *DIN 15020-1:1974-02*; Lift Appliances; Principles Relating to Rope Drives; Calculation and Construction. DIN: Berlin, Germany, 1974.
23. *EN 10025+A1:1994*; Produtos Laminados a Quente de Aços de Construção Não Ligados. Instituto Português da Qualidade: Caparica, Portugal, 1994.
24. *EN 10083-3:2006*; Steels for Quenching and Tempering—Part 3: Technical Delivery Conditions for Alloy Steels. European Committee for Standardization: Brussels, Belgium, 2006.
25. *ANSI/CEMA B105.1-2015*; Specifications for Welded Steel Conveyor Pulleys with Compression Type Hubs. ANSI/CEMA: Washington, DC, USA, 2015.
26. Shigley, J.E. *Mechanical Engineering Design*, 3rd ed.; McGraw-Hill Kogakusha: Tokyo, Japan, 1977.
27. The Engineering ToolBox. Brinell Hardness Number BHN. Available online: https://www.engineeringtoolbox.com/bhn-brinell-hardness-number-d_1365.html (accessed on 26 December 2022).
28. Shigley, J.E. *El Proyecto en Ingeniería Mecánica*; Ediciones del Castillo SA: Madrid, Spain, 1970.